

Conformationally Constrained Peptide Analogues of pTyr-Glu-Glu-Ile as Inhibitors of the Src SH2 Domain Binding

Nguyen-Hai Nam,[†] Guofeng Ye,[†] Gongqin Sun,[#] and Keykavous Parang^{*,†}

Department of Biomedical Sciences and Department of Cell and Molecular Biology, University of Rhode Island, Kingston, Rhode Island 02881

Received January 13, 2004

A series of conformationally constrained peptides were designed and synthesized as the Src SH2 domain ligands based on a tetrapeptide sequence pTyr-Glu-Glu-Ile (pYEEI). In general, the constrained peptides such as compounds **6**, **7**, and **11** ($IC_{50} = 1.1\text{--}1.5\ \mu\text{M}$) showed higher binding affinities to the Src SH2 domain relative to the corresponding linear peptides **8a**, **9a**, and **13a**, respectively ($IC_{50} > 100\ \mu\text{M}$), and pYEEI ($IC_{50} = 6.5\ \mu\text{M}$), as evaluated by a fluorescence polarization assay. Molecular modeling studies revealed that in constrained peptides, the isoleucine side chain penetrates very deeply into the hydrophobic binding pocket (P + 3 site) of the Src SH2 domain. These constrained peptides can serve as novel templates for the design of small and nonpeptidic inhibitors of the Src SH2 domain.

Introduction

The pp60^{c-Src} (Src) protein is a nonreceptor tyrosine kinase that is characterized by an N-terminal unique domain followed by two Src homology domains SH3 and SH2, a kinase domain, and a short C-terminal regulatory peptide segment. Src has been implicated to play a role in both breast cancer¹ and osteoporosis,^{2,3} suggesting that it might be an attractive therapeutic target. SH2 domains consist of approximately 100 amino acids and bind to phosphotyrosine-containing proteins, such as middle T antigen, PDGF receptor, EGF receptor, and focal adhesion kinase,^{1,4–7} in a sequence-dependent manner.

Considerable efforts have been devoted to the development of the Src SH2 domain inhibitors. Most of the reported small-molecule inhibitors resulted from a rational drug design approach based on a pTyr-Glu-Glu-Ile (**1**, pYEEI, Figure 1) peptide template, which was shown to be the optimal binding sequence for the Src SH2 domains of the Src family of kinases.⁸ The crystal structure of pYEEI in complex with the Src SH2 domain reveals a very characteristic binding mode that can be described as a two-pronged plug engaging a two-hole socket. The Src SH2 domain has two major interaction sites with pYEEI, i.e., the hydrophilic phosphotyrosine binding pocket (P site) and the hydrophobic pocket (P + 3 site). The phosphotyrosine residue of pYEEI is buried in the deep positively charged pocket (P site). The isoleucine (I) residue intrudes into the hydrophobic pocket (P + 3 site). The EE motif lies across the flat surface of the protein, has little interaction with the protein framework, and plays a role of a linker delivering the two residues pY and I to respective binding

pockets.^{9–11} Indeed, a variety of heterocyclic systems have been shown to be effective surrogates for the EE motif.^{12–16}

Cyclization strategy has been proved to be very useful in developing diagnostically and therapeutically peptidic and peptidomimetic agents.^{17–19} Since peptides generally adopt highly flexible conformations in solution, a cyclization approach has been commonly used to reduce the conformational freedom of these molecules. Conformationally constrained structures are more selective in their affinity toward specific receptors and more stable toward proteases. In addition, cyclization often results in higher receptor binding affinity possibly by reducing unfavorable entropic effects.

Introducing conformational constraints into flexible ligands has been used as a strategy for the design of new ligands having higher binding affinity for SH2 domains.^{20,21} Several compounds, such as **2** and **3** (Figure 1), have emerged from these efforts and have been shown to have in vivo activity.^{22,23} Since Arg158 of the Src SH2 domain interacts with the carbonyl group of the N-acetylated tyrosine residue of pYEEI,^{9–11} the modification of N-terminal group of pYEEI was not considered for designing peptidomimetics in several of these earlier efforts.^{22,23}

We envisaged that cyclization of the γ -carboxylic acid of the P + 1 Glu (the amino acid adjacent to pY) or P + 2 Glu (the amino acid adjacent to Ile) with the N-terminal in pYEEI might produce constrained ligands (**4–7**, **10**, **11**, Figure 2) with higher binding affinity for the Src SH2 domain. These carboxylic acids are not involved in major interactions with two major binding pockets (P and P + 3 sites) of the Src SH2 domain as shown in parent peptide **1**.^{9,10} This general design approach was used to synthesize more rigid ligands and to generate additional favorable hydrogen bonding with amino acids in the binding pocket of the Src SH2 domain. Constrained peptides (**4–7**, **10**, **11**) have lactam carbonyl groups instead of one of the carboxylic acid

* To whom correspondence should be addressed. Phone: +1-401-874-4471. Fax: +1-401-874-5048. E-mail address: kparang@uri.edu.

[†] Department of Biomedical Sciences.

[#] Department of Cell and Molecular Biology.

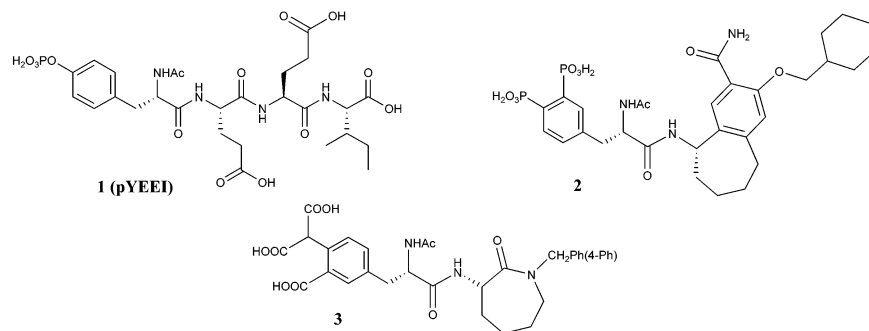


Figure 1. Structures of pYEEI (pTyr-Glu-Glu-Ile) and two peptidomimetics as Src SH2 domain inhibitors.

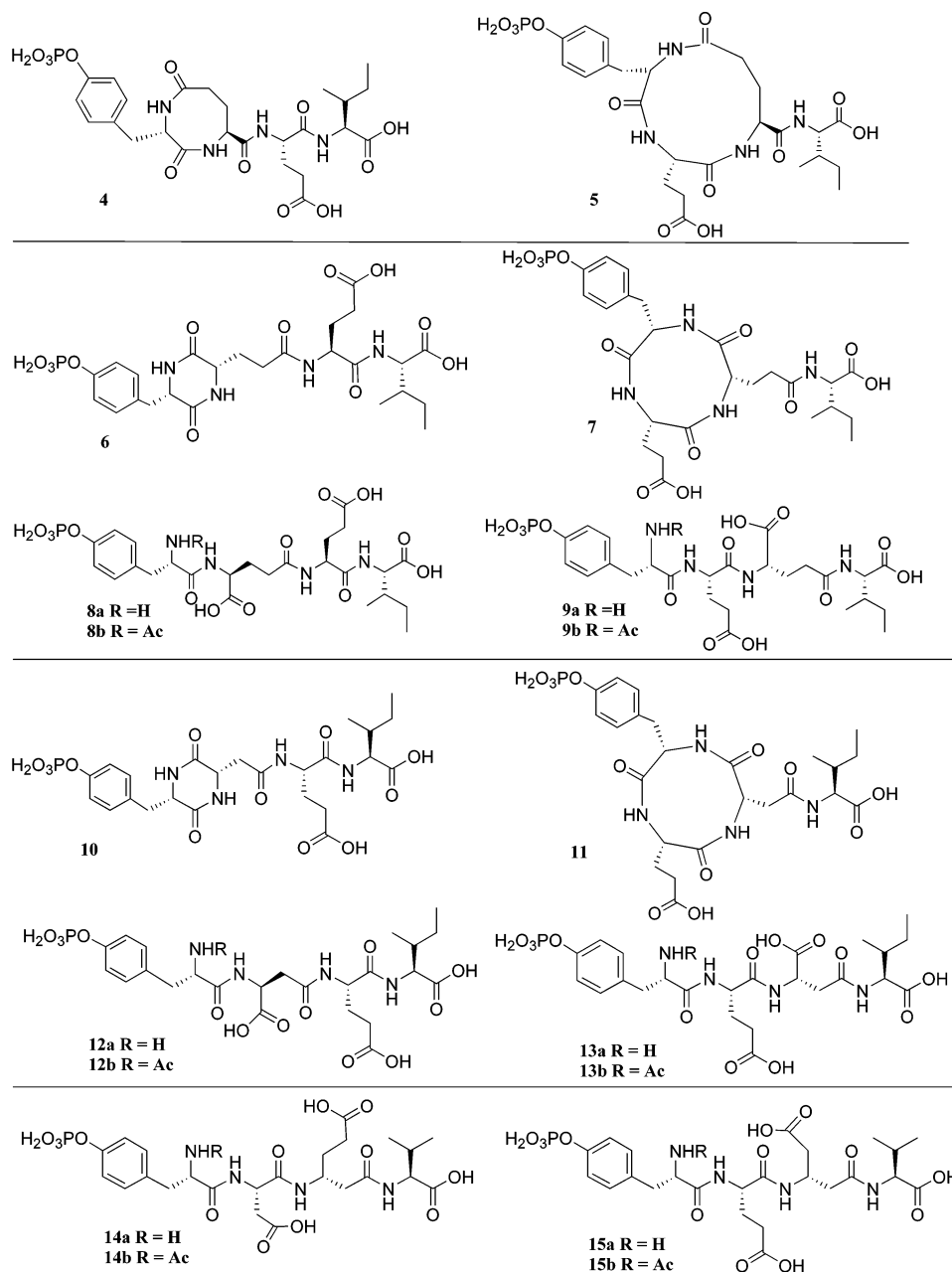


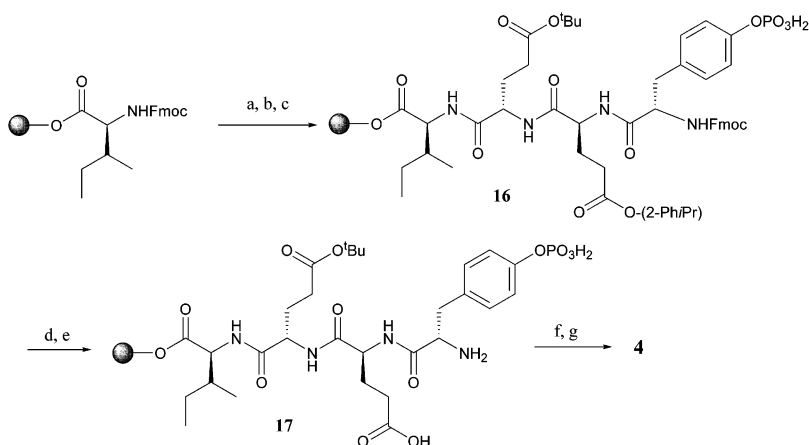
Figure 2. Structures of the constrained peptide analogues of pYEEI and the corresponding linear peptides.

groups of glutamic acid in pYEEI. In all constrained peptides, one carboxylic acid remained unchanged to minimize any radical structural modifications. No structural modifications were made in phosphotyrosine and isoleucine residues; therefore, the conformations adopted by constrained peptides correspond to the original

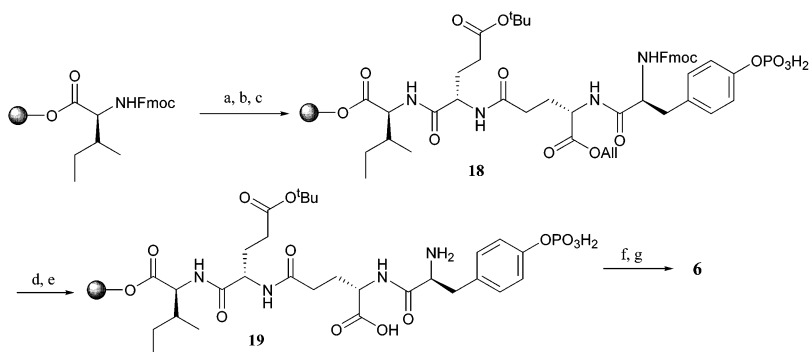
parent peptide, pYEEI, with respect to the binding to two major binding pockets.

Chemistry

Figure 2 displays the chemical structures of the synthesized constrained and the corresponding linear

Scheme 1^a

^a Reagents: (a) (i) piperidine 20%/DMF; (ii) Fmoc-Glu(*t*Bu)-OH, HBTU, NMM, DMF; (b) (i) piperidine 20%/DMF; (ii) Fmoc-Glu(O-2-Ph/Pr)-OH, HBTU, NMM, DMF; (c) (i) piperidine 20%/DMF; (ii) Fmoc-Tyr(PO₃H₂)-OH, HBTU, NMM, DMF; (d) TFA/DCM/TIPS (1:95:4); (e) piperidine 20%/DMF; (f) HBTU, NMM, DMF (24 h); (g) TFA/anisole/H₂O (90:5:5).

Scheme 2^a

^a Reagents: (a) (i) piperidine 20%/DMF; (ii) Fmoc-Glu(*t*Bu)-OH, HBTU, NMM, DMF; (b) (i) piperidine 20%/DMF; (ii) Fmoc-Glu-OAll, HBTU, NMM, DMF; (c) (i) piperidine 20%/DMF; (ii) Fmoc-Tyr(PO₃H₂)-OH, HBTU, NMM, DMF; (d) Pd(PPh₃)₄, CHCl₃/AcOH/NMM (37:2:1); (e) piperidine 20%/DMF; (f) HBTU, NMM, DMF (2 × 1.5 h); (g) TFA/anisole/H₂O (90:5:5).

peptides. All final compounds were purified using HPLC and characterized by spectroscopic methods (¹H NMR, HRMS). The peptides were assembled on solid phase (Wang resin) using a standard Fmoc peptide protocol with HBTU/NMM as coupling reagents.

To synthesize compound **4**, Fmoc-Glu(O-2-Ph/Pr)-OH (*N*-α-Fmoc-L-glutamic acid γ -2-phenylisopropyl ester), a quasi-orthogonally protected Glu derivative, was assembled at the P + 1 position in the peptide sequence to yield **16**. The γ -2-phenylisopropyl (2-Ph/Pr) protecting group in resin-bound peptide **16** was selectively removed using TFA/DCM (1%) to give **17** (Scheme 1). Initial cyclization of **17** using HBTU (2 × 1.5 h, 8 equiv each time) failed to yield **4** after cleavage. However, increasing the coupling time to 24 h followed by cleavage furnished **4** in an overall yield of 15%. Prolongation of the reaction time to 48 h did not improve the yield. Instead, a significant amount of guanidinium side product was formed as a result of the reaction between HBTU and the N-terminal amino group, together with YEEI formed as a result of the hydrolysis of the phosphate group. The constrained peptide **4** was purified using HPLC and characterized by spectroscopic methods.

A similar strategy was applied for the synthesis of **5**, with Fmoc-Glu(O-2-Ph/Pr)-OH assembled at the P + 2 position in the tetrapeptide sequence. However, cyclization of the N-terminal amino group with the γ -carboxylic

acid in the P + 2 Glu moiety by HBTU proved to be less efficient; only a trace of the cyclic product was observed, together with a large peak attributed to the guanidinium side product, as examined by HPLC. Further attempts to cyclize the P + 2 γ -carboxylic and the N-terminal amino group by BOP-Cl or PyBOP failed to give **5** in a significant yield. However, the use of DPPA (10 equiv, 24 h) afforded **5** in ca. 11% yield after cleavage from the resin (Scheme 3; see Materials and Methods).

To further explore the effect of cyclization on the binding affinity, two cyclic variants (**6**, **7**) of the two γ -glutamyl pYEEI analogues were also synthesized. To synthesize **6**, Fmoc-Glu-OAll, an orthogonally protected Glu derivative, was assembled at the P + 1 position in the tetrapeptide sequence to yield **18** (Scheme 2). The β -carboxylic group in resin-bound peptide **18** was unmasked with Pd(PPh₃)₄ (2.5 equiv) in CHCl₃/AcOH/NMM (37:2:1) to give **19**. Cyclization of **19** was carried out efficiently using HBTU/NMM (2 × 1.5 h, 4 equiv each time) as coupling reagent to afford **6** in a moderate overall yield after cleavage (41%). A similar strategy was applied for the synthesis of **7**, with Fmoc-Glu-OAll assembled at the P + 2 position in the peptide sequence. However, cyclization between the γ -carboxylic and the N-terminal amino groups did not proceed with either HBTU or BOP reagent. The cyclic peptide **7** was synthesized using DPPA (20 equiv, 2 × 24 h) as the

Table 1. Binding Affinity of the Synthesized Compounds for the Src SH2 Domain

compd	binding affinity ^a	compd	binding affinity ^a
1	6.5	11	1.5
4	3.3	12a	>100
5	5.9	12b	75.4
6	1.2	13a	>100
7	1.1	13b	90.7
8a	>100	14a	83.2
8b	69.5	14b	34.6
9a	>100	15a	76.3
9b	80.7	15b	25.7
10	12.1		

^a IC₅₀ (μM): concentration that inhibits the binding of the fluorescent probe (fluoresceinated GpYEEI; see Materials and Methods) to the Src SH2 domain by 50%. The reported IC₅₀ values are the mean of three separate determinations with a standard deviation of less than ±5%.

coupling reagent though in a low yield (ca. 7% based on the resin after cleavage) (Scheme 4; see Materials and Methods). This cyclization method did not result in significant racemization (less than 5%). Two other cyclic derivatives (**10**, **11**) and corresponding linear peptides, pTyr-β-Asp-Glu-Ile (**12a**) and pTyr-Glu-β-Asp-Ile (**13a**), were also synthesized using Fmoc-Asp-O-All instead of Fmoc-Glu-OAll in a similar strategy, though in low yields (7–10%). The difficulty in cyclization of short peptides has been reported¹⁸ to be due to a strong π-character and preferential trans conformation of the peptide bonds, which places the carboxylic and amine termini in remote positions unfavorable for cyclization. Several approaches employing photolabile auxiliaries in ring contraction have been explored.^{24–28} It is expected that application of these approaches may lead to higher overall yields of the present conformationally constrained peptides.

The polarities of constrained peptides were compared with the corresponding linear peptides using the LogKow (KowWin) program, which estimates the log of the octanol/water partition coefficient (log *P*) of organic chemicals using an atom or fragment contribution method. The data indicated that there were no significant changes in the polarity of constrained peptides compared to the corresponding linear compounds. For example, the LogKow for pYEEI (−0.77) was comparable to that of compound **5** (−0.82). Similarly, the LogKow value for linear peptide **13a** (−1.78) was comparable to that of the corresponding constrained peptide **11** (−1.31).

Results and Discussion

The binding affinities of the synthesized constrained peptides against the Src SH2 domain were examined and compared with the corresponding linear tetrapeptides using a fluorescence polarization competitive assay.^{29,30} The results expressed as IC₅₀ values are shown in Table 1. The Insight II molecular modeling program was used to simulate the interactions of constrained peptides with binding site amino acids. Cyclization of the P + 1 γ-carboxylic and the N-terminal amino groups proved to be beneficial for the binding affinity, with compound **4** (IC₅₀ = 3.3 μM) being 2-fold more potent than pYEEI (IC₅₀ = 6.5 μM) as a ligand for the Src SH2 domain. Arg158 of the Src SH2 domain interacts with the carbonyl group of the N-acetylated tyrosine resi-

due.^{9–11} This interaction is lost in compound **4**, which lacks an N-acetylated group. Molecular modeling studies using the minimized structure of compound **4** in the binding pocket of the Src SH2 domain indicate the formation of hydrogen bonding between the His204(NH) backbone and the oxygen of the lactam carbonyl group (see Figure 3a). This hydrogen bonding may be involved in increasing the binding affinity of compound **4**. The potentiating effect of conformational constraint in this peptide might be explained by allowing the phosphotyrosine to adopt a more optimal conformation to form a more favored bond network within the phosphotyrosine binding pocket. In the case of pYEEI, the minimized crystal structure of its complex with the Src SH2 domain shows a separation of 16.35 and 16.84 Å between the phosphorus atom of the P tyrosine residue (pYEEI:B101H:P) and methyl (pYEEI:B104:CD) and carbonyl (pYEEI:B104:C) groups of the P + 3 isoleucine, respectively, which is considered an optimal range. This feature can be seen in other potent inhibitors crystallized with the Src kinases SH2 domain. The study of these crystal structures (1ISO, 1FBZ, 11JR)^{20,23,31} revealed that the separation of phosphorus atom and the terminal carbon is in the range 16.43–16.89 Å, which is close to that of pYEEI, indicating the importance of separation between phosphotyrosine or phosphotyrosine mimics and hydrophobic groups for interaction with P and P + 3 sites, respectively. The distances between the phosphorus atom of the phosphotyrosine residue and the carbon atoms of the terminal methyl and carbonyl of isoleucine in compound **4** were 15.60 and 16.95 Å, respectively, which allows for appropriate interaction of these functional groups with P and P + 3 binding pockets (Figure 3b).

Compound **5** did not improve the binding affinity significantly (IC₅₀ = 5.9 μM). Molecular modeling studies using the minimized structure of compound **5** showed the formation of favorable hydrogen bondings between the lactam carbonyl group and the carboxylic acid of glutamic acid (P + 1) [Glu-B102(OE2)] with Arg158:HH22 and HisA204(NH), respectively. On the other hand, cyclization reduced the hydrophobic interaction of the isoleucine side chain with the hydrophobic pocket because of overall contraction of the peptide. The isoleucine side chain of compound **5** forms extended contacts with the pY + 3 pocket, although it does not extend as deeply into the pY + 3 pocket as the Ile side chain of pYEEI. In fact the isoleucine side chain is positioned outside the hydrophobic binding pocket (Figure 4). The phosphotyrosine and isoleucine are brought into proximity as they bind to the Src SH2 domain. The distances between phosphorus atom of the phosphotyrosine residue and the carbon atom of isoleucine carbonyl is 11.91 Å, which is significantly shorter than the corresponding distances in pYEEI and compound **4**.

The constrained diketopiperazine peptide analogue **6** exhibited a higher binding affinity (IC₅₀ = 1.2 μM) for the Src SH2 domain than the constrained peptides, **4** and **5**, and pYEEI. Similarly, compound **7**, which has a two-carbon linker separating the ring system and the Ile moiety, showed 5-fold higher binding affinity (IC₅₀ = 1.1 μM) than pYEEI. Interestingly, the corresponding linear peptides **8a** and **9a** did not show any

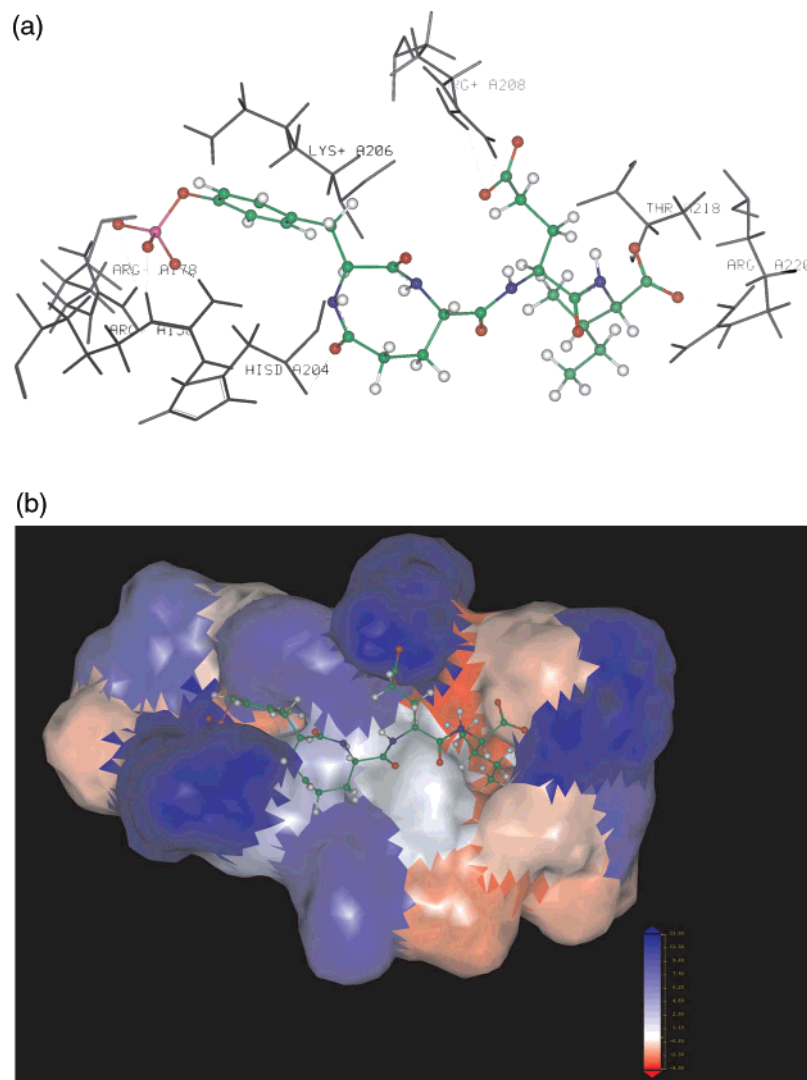


Figure 3. (a) Major interactions of constrained peptide **4** with amino acids of the Src SH2 domain. Compound **4** and side chains of amino acids of the Src SH2 domain are represented by ball-and-stick vectors and sticks, respectively. The carbon skeleton of compound **4** is green, hydrogens are white, oxygen atoms are red, nitrogens are blue, and the phosphorus atom is cyan. The key amino acid residues within the pTyr-binding pocket of the Src SH2 protein are labeled. The binding pocket amino acids (sticks, cyan, white) form hydrogen bonds with different functional groups of peptide. (b) Molecular surface rendering of the compound **4**-Src SH2 domain. Compound **4** is represented by ball-and-stick vectors and interacts with P and P + 3 sites of the Src SH2 domain, respectively. The protein is represented on the basis of the hydrophobicity characteristics of the different sites with red for the highest hydrophobic amino acids. The figure is drawn using the Accelrys visualization system.

significant binding at the maximum concentration of 100 μM . The interaction of compound **7** with the SH2 domain of Src is shown in Figure 5. The phosphate group forms salt bridges to the side chains of Arg158 and Arg178. Deep hydrophobic interactions exist between the isoleucine side chains and the P + 3 site. The molecular modeling studies indicated that for both peptides **6** (16.60 Å) and **7** (16.10 Å) distances between the phosphorus atom and the carbon atom of isoleucine carbonyl were in the optimal range, allowing the proper orientation of the constrained peptide for interaction with the P and P + 3 binding pockets. Similarly the distances between the phosphorus atom and the terminal methyl group of isoleucine for peptides **6** (15.42 Å) and **7** (16.16 Å) were in the optimal range. Constrained peptide **6** showed a hydrogen bond between HisA204-(NH) and one of the lactam carbonyl groups. Constrained peptide **7** showed a hydrogen bond between HisA204(CO) and the lactam amino group (NH). An

interesting feature for peptide **7** is the formation of hydrogen bonding between the carboxylic acid of glutamic acid (GluB102:OE1) and the phenolic hydroxyl group of Tyr205 (TyrA205:OH) (Figure 5). The formation of this hydrogen bonding might allow the phosphate group of phosphotyrosine to have a stronger interaction with positively charged amino acids in the P site. A comparison of compounds **6** and **7** with the pYEEI peptide shows that both compounds display the same binding mode. Compared to the isoleucine side chain in the pYEEI peptide, the isoleucine side chain in compound **6** fits better in the hydrophobic pocket. In the corresponding peptides **8a** and **9a** ($\text{IC}_{50} > 100 \mu\text{M}$), the separation between the phosphorus atom of phosphotyrosine and the carbonyl group of isoleucine was shorter (**8a**, 14.34 Å) or longer (**9a**, 18.35 Å) than the optimal range. Similar results were obtained for distances between the phosphorus atom of phosphotyrosine and the terminal methyl group of isoleucine for **8a** (13.63 Å) and **9a** (18.86

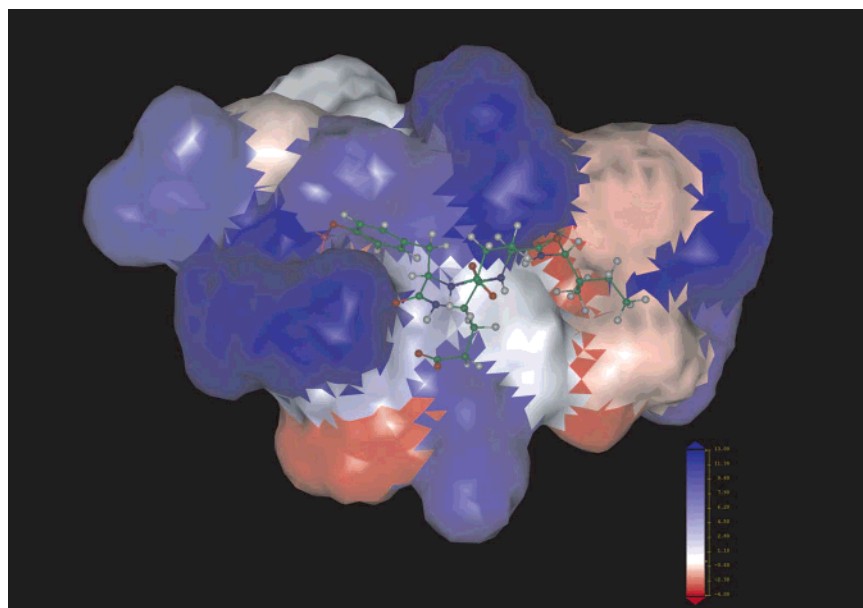


Figure 4. Predicted binding mode of compound **5** (ball-and-stick model) with Src SH2 (surface). The carbon skeleton of compound **5** is green, hydrogens are white, oxygen atoms are red, nitrogens are blue, and the phosphorus atom is cyan. The protein is represented on the basis of the hydrophobicity characteristics of the different sites with red for the highest hydrophobic amino acids. The figure is drawn using the Accelrys visualization system.

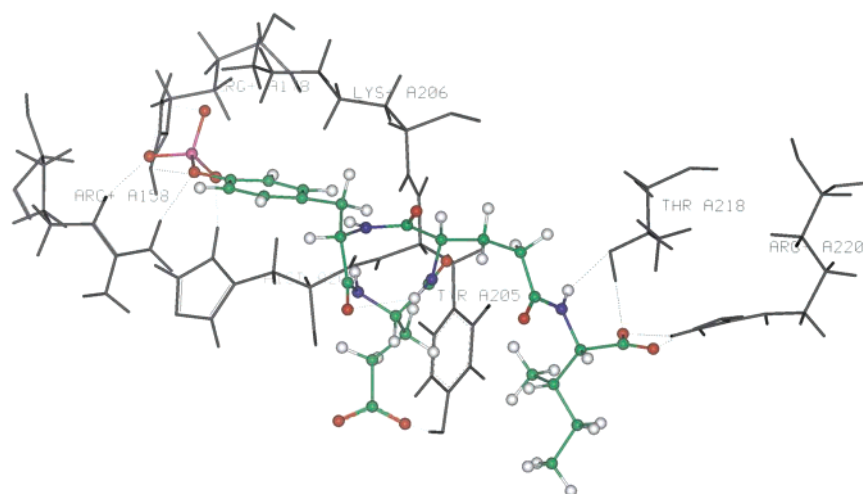


Figure 5. Major interactions of constrained peptide **7** with amino acids of the Src SH2 domain. Compound **7** and the side chains of amino acids of the Src SH2 domain are represented by ball-and-stick vectors and sticks, respectively. The key amino acid residues within the pTyr-binding pocket of Src SH2 protein are labeled. The binding pocket amino acids (sticks, white) form hydrogen bonds with different functional groups of peptide. The carbon skeleton of compound **7** is green, hydrogens are white, oxygen atoms are red, nitrogens are blue, and the phosphorus atom is cyan.

Å). Peptides **8a** and **9a** are not acetylated; therefore, there was no such interaction of the carbonyl of the acetyl group with Arg158 of the Src SH2 domain as observed in Ac-pYEEI. The corresponding acetylated compounds (**8b**, $IC_{50} = 69.5 \mu M$) and (**9b**, $IC_{50} = 80.7 \mu M$) did not improve the binding affinity significantly, indicating that the cyclization in constrained peptides **6** and **7** was the major factor in improving binding affinity to the Src SH2 domain.

Similarly, the binding affinity of the constrained peptides **10** ($IC_{50} = 12.1 \mu M$) and **11** ($IC_{50} = 1.5 \mu M$) were at least 10- and 100-fold higher than that of nonacetylated **12a** and **13a** ($IC_{50} > 100 \mu M$), respectively. Linear N-acetylated derivatives of compounds **12b** ($IC_{50} = 75.4 \mu M$) and **13b** ($IC_{50} = 90.7 \mu M$) were more active than nonacetylated compounds **12a** and **13a**, but acetylation was not enough to explain the much

higher binding affinity of the corresponding constrained peptides **10** and **11**. Molecular modeling studies revealed that the lactam carbonyl or amino groups form hydrogen bonds with the side chain of His204. One of the lactam carbonyl groups in peptide **10** formed a hydrogen bond with the HisA204:NH group. One of the lactam amino groups (NH) in peptide **11** forms a hydrogen bond with the carbonyl of HisA204:O. As observed for constrained peptide **7**, the carboxylic acid of glutamic acid (Glu-B102:OE1) in compound **11** forms an unexpected hydrogen bond with the phenolic hydroxyl group of tyrosine (TyrA205:OH). These interactions stabilize the favorable backbone conformation of the constrained peptides for other residues such as phosphotyrosine and isoleucine to interact effectively with the protein and also lock the side chain conformation of these residues with a favorable entropic contribu-

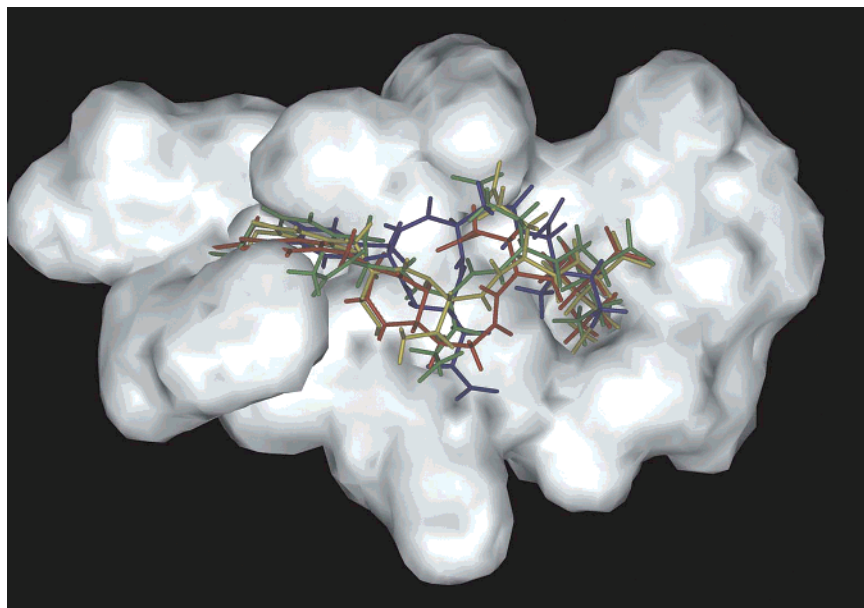


Figure 6. Comparison of the structural complexes of the Src SH2 domain with different constrained peptides (pYEEI, green; compound **4**, yellow; compound **6**, red; compound **11**, blue) based on molecular modeling. The peptides are rendered in ball-and-stick styles. They are the lowest energy conformers predicted for constrained peptides.

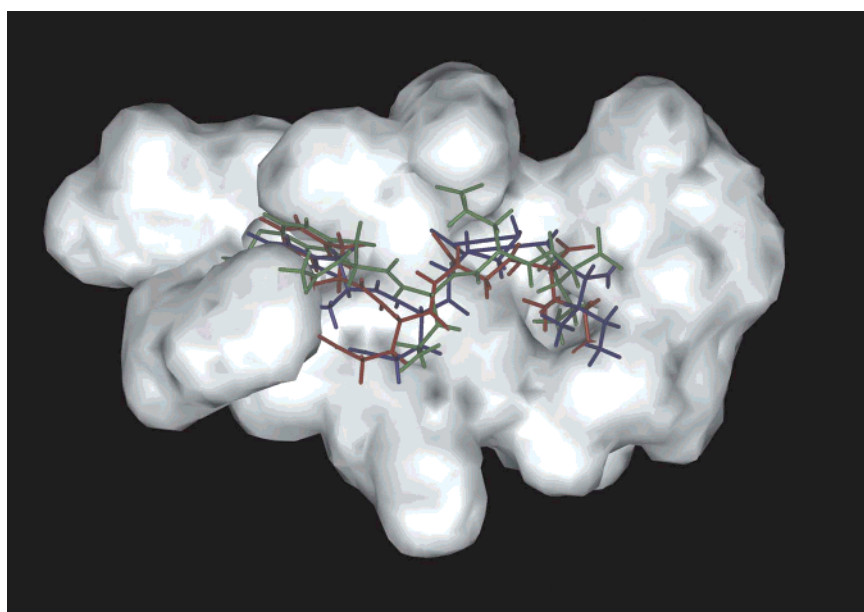


Figure 7. Comparison of the structural complexes of the Src SH2 domain with different linear peptides (pYEEI, green; compound **9**, blue; compound **13**, red) based on molecular modeling. The peptides are rendered in ball-and-stick styles. They are the lowest energy conformer predicted for constrained peptides.

tion. In the corresponding linear peptides **12a** and **13a** ($IC_{50} > 100 \mu M$), the separation between the phosphorus atom of phosphotyrosine and the carbon atom of isoleucine carbonyl (**12a**, 15.59 Å; **13a**, 15.52 Å) was shorter than that of pYEEI (16.84 Å). Similarly the distance between the phosphorus atom of phosphotyrosine and terminal methyl group of tyrosine in **12a** (14.79 Å) was shorter than that of pYEEI (16.35 Å). This suggests that the distance between the phosphate and the side chain group of isoleucine is an essential feature for high-affinity inhibitor binding and only limited deviations for this distance are tolerated. Several important hydrogen bonds are lost in the linear nonconstrained peptides. In addition, the side-chain-flexible glutamic acid is less favored than the rigid ring, considering the entropic penalty in the process of

binding. Similarly, the corresponding acetylated compounds **12b** and **13b** did not improve the binding affinity significantly. Binding affinities for four other linear control peptides (**14a**, **14b**, **15a**, **15b**; $IC_{50} = 25.7-83.2 \mu M$) were not comparable to all synthesized constrained peptides (**4-7**, **10**, **11**; $IC_{50} = 1.1-12.1 \mu M$).

The isoleucine side chains in constrained peptides, such as **4**, **6**, **10**, and **11**, reach fairly deeply in the P + 3 site pocket (Figure 6), while those in other corresponding linear compounds, such as **9** and **13**, are not able to penetrate very deeply into the pocket (Figure 7). The charged phosphate group is able to interact with Arg158 and Arg178 in different ways. In some peptides (**6**, **8**) two terminal oxygen atoms only form salt bridges to both arginines. However, in most peptides (**4**, **5**, **9-12**), two terminal and one ester oxygen or three

terminal oxygens of the phosphate group form hydrogen bonds with Lys206, Arg178, and Arg158, forcing the phenyl ring in a different conformation. In addition to salt bridges with Arg158 and Arg178, the charged phosphate groups in compounds **7**, **9–11**, and **13** form additional hydrogen bonds with aromatic amino group of His204. It remains to be seen whether different modes of interaction of the phosphate group of phosphotyrosine with positively charged amino acids in the P site of the Src SH2 domain have any direct influence on the binding affinity of these analogues.

In summary, the synthesis and evaluation of constrained peptides such as the Src SH2 domain ligands based on the tetrapeptide pYEEI sequence were undertaken to explore their mode of interaction with the binding pocket amino acids. This study revealed a number of important and interesting features regarding the design of conformationally constrained peptide mimics. The presence of the constrained ring had a dramatic effect on the binding of the inhibitors described in this report, enhancing the affinity significantly over the acyclic analogues. In the case of corresponding linear peptides, the separation between the phosphorus atom of phosphotyrosine and the carbonyl group and the terminal methyl of isoleucine is either shorter or longer, preventing interaction of the isoleucine side chains deep in the P + 3 site and the optimal interaction of phosphate group with positively charged amino acids in the P site of the Src SH2 domain. The distances between the phosphorus atom of phosphotyrosine and the terminal methyl group of isoleucine for constrained peptides (**6**, **7**, **11**; 15.42–16.18 Å) were comparable to that of pYEEI (16.35 Å). These constrained peptides may offer novel templates for further design of the Src SH2 domain inhibitors and in turn provide a conceptual approach toward the design of SH2 domain directed peptidomimetics. A wide variety of substituents mimicking Ile and phosphotyrosine functional groups have been reported.^{32–34} Incorporation of these structural features into the cyclic templates reported here may produce a novel class of small, nonpeptidic inhibitors of the Src SH2 domain. It remains to be seen whether the introduction of these conformational constraints will reduce the conformational entropy penalty upon receptor binding, resulting in a net gain in the free energy of binding. Clearly, further structural and thermodynamic studies would be required for more detailed analyses.

Materials and Methods

1. Expression and Purification of Src SH2 Domain.

One 300 mL culture of *E. coli* (strain TGI) containing pGEX-2T in YT broth with 100 µg/mL ampicillin was prepared and allowed to incubate with shaking at 37 °C overnight (Innova 2000 Platform Shaker, New Brunswick Scientific, 200 rpm). A fresh 300 mL YT broth containing 100 µg/mL ampicillin was mixed with the overnight culture, induced with 0.2 mM isopropylthiogalactoside (IPTG), and incubated at room temperature with shaking for 5 h. The cells were harvested by centrifugation at 5000g for 5 min. The supernatant was discarded, and the cell pellet was resuspended in 5 mL of 1X PBS buffer (0.1% β-mercaptoethanol). The cell lysis was carried out via sonication (three separate 10 s bursts, with 30 s incubations on ice between each burst). The lysate was centrifuged at 15000g for 20 min, and the supernatant was added to a 4 µM slurry of glutathione-S-transferase (GST) in 1X PBS buffer (0.1% β-mercaptoethanol). The protein was released from the GST affinity column by the addition of 5

mL of reduced GST (0.1% β-mercaptoethanol) and detected by 5X Bradford reagent. The concentration of protein was determined by reading optical density employing a Pharmacia Biotech Ultrospec 2000 UV/vis spectrophotometer using bovine serum albumin (BSA, 1.0 mg/mL) as a standard.

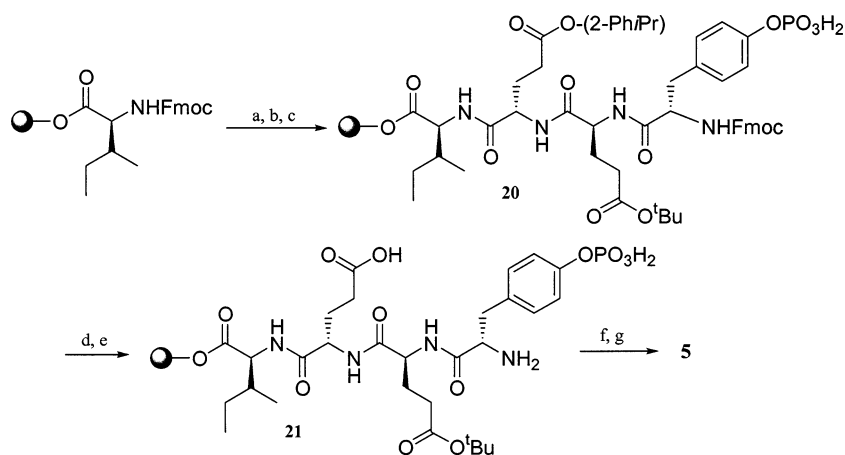
2. Src SH2 Domain Binding Assay. All peptides were tested as competitors against the fluorescent probe for binding affinity to the Src SH2 domain using a fluorescent polarization (FP) competitive binding assay as described below. FP was measured at 25 °C in a disposable glass tube (volume, 600 µL) using a Perkin Elmer LS 55 luminescence spectrometer equipped with an FP apparatus. The excitation and emission wavelengths were set at 485 and 535 nm, respectively. For the competition assay, final concentrations of 750 nM SH2, 80 nM fluorescent probe, phosphate buffer (20 mM, pH 7.3, 100 mM NaCl, 2 mM DTT, 0.1% BSA), water, and various concentrations (0–10 mM) of each competitor peptide were used. The assay was designed so that the concentration of competing peptide in any tube was doubled relative to that of the previous tube. The order of addition to each 600 µL glass tube was (i) buffer, (ii) water, (iii) fluorescent probe, (iv) SH2 domain, and (v) competitor peptide. A blank control (with the Src SH2 domain but without a peptide) and a background control (without both the Src SH2 domain and the peptide) were used. The inhibition percentage (IP) of fluorescent probe binding to the Src SH2 domain by the sample was calculated by the following equation:

$$\left(1 - \frac{\text{FP}_{\text{blk}} - \text{FP}_s}{\text{FP}_{\text{blk}} - \text{FP}_{\text{bgd}}}\right) \times 100$$

where FP_{blk} is the fluorescent polarization value of the blank control, FP_s is the fluorescent polarization value of the sample (peptide), and FP_{bgd} is the fluorescent polarization value of the background control. The inhibition percentages of the various concentrations of the assayed peptides were plotted, and the IC_{50} value (a concentration that inhibits the binding of the fluorescent probe to the Src SH2 domain by 50%) was calculated using the CurveExpert 6.0 software. The reported IC_{50} values are the mean of three separate determinations with a standard deviation of less than ±5%.

3. Molecular Modeling. Simulations were performed with the Accelrys Insight II 2000/Discover 97 modeling package, with the cff91 forcefield. Models were constructed on the basis of the X-ray crystal structure of the Ac-pYEEI peptide bound to the Src-SH2 domain from the Protein Data Bank (1SHD). The positions of the backbone atoms and of the side chain atoms were identical with those of Ac-pYEEI. The remaining residues of constrained peptides were subsequently added to or built on this minimized model. During minimization all atoms were held fixed except for the peptide and binding site residues within 5 Å of the peptide. For refinement, the peptide/receptor complex first underwent 50 steps of steepest descent and 150 steps of conjugate gradient minimization. Next, the complex was equilibrated briefly with 10 molecular dynamics runs of 200 steps each at 300 K. Velocities were reassigned to a random Boltzmann distribution for each run. The final structure was then minimized with 300 steps with the conjugate gradient algorithm.

4. General Synthesis and Purification of Peptides. In general, all peptides were synthesized by the solid-phase peptide synthesis strategy on a PS3 automated peptide synthesizer (Rainin Instrument Co., Inc.) employing *N*-(9-fluorenyl)methoxycarbonyl (Fmoc) based chemistry on 0.1 mmol of Fmoc-Ile-Wang resin (loading capacity, 0.56 mmol/g). 2-(1*H*-Benzotriazole-1-yl)-1,1,3,3-tetramethyluronium hexafluorophosphate (HBTU)/1-hydroxybenzotriazole (HOBt) (0.4 mmol) and NMM (0.4 M) in *N,N*-dimethylformamide (DMF) were used as coupling and activating reagents, respectively. Fmoc-Ile-Wang resin (0.1 mmol, 179 mg, 0.56 mmol/g), coupling reagents (0.4 mmol), and Fmoc-amino acid building blocks (0.4 mmol), including Fmoc-Tyr(PO_3H_2)-OH, Fmoc-Glu(*t*Bu)-OH, Fmoc-Glu(Ph/Pr)-OH, and Fmoc-Glu-OAll, were purchased from Novabiochem. Fmoc deprotection at each step

Scheme 3^a

^a Reagents: (a) (i) piperidine 20%/DMF; (ii) Fmoc-Glu(O-2-Ph/Pr)-OH, HBTU, NMM, DMF; (b) (i) piperidine 20%/DMF; (ii) Fmoc-Glu(tBu)-OH, HBTU, NMM, DMF; (c) (i) piperidine 20%/DMF; (ii) Fmoc-Tyr(PO₃H₂)-OH, HBTU, NMM, DMF; (d) TFA/DCM/TIPS (1:95:4); (e) piperidine 20%/DMF; (f) DPPA (10 equiv, 24 h); (g) TFA/anisole/H₂O (90:5:5).

was carried out using 20% piperidine/DMF. A mixture of TFA/anisole/water (95:2.5:2.5) was used for side chain deprotection of amino acids and cleavage of the synthesized peptides from the resin. Crude peptides were precipitated by addition of cold diethyl ether (Et₂O) and purified by HPLC (Shimadzu LC-8A preparative liquid chromatograph; Shimadzu fraction collector 10A) on a Phenomenex Prodigy 10 μm ODS reversed-phase column. Peptides were separated by eluting the crude peptide at 4.0 mL/min using a gradient of 0–100% acetonitrile (0.1% TFA) and water (0.1% TFA) over 85 min and were lyophilized. The purity of final products (>95%) was confirmed by analytical HPLC on a Shimadzu 3 μm C-18 column at 0.5 mL/min using the same gradient system. The chemical structures of compounds were confirmed by a high-resolution PE Biosystems Mariner API time of flight mass spectrometer and NMR. ¹H NMR and ¹³C NMR spectra were recorded at 400 MHz on a Bruker 400 spectrometer with tetramethylsilane as an internal standard using CD₃OD as a solvent. Chemical shifts are reported in parts per millions (ppm). Details of cyclization procedures and spectroscopic data of representative compounds are presented below.

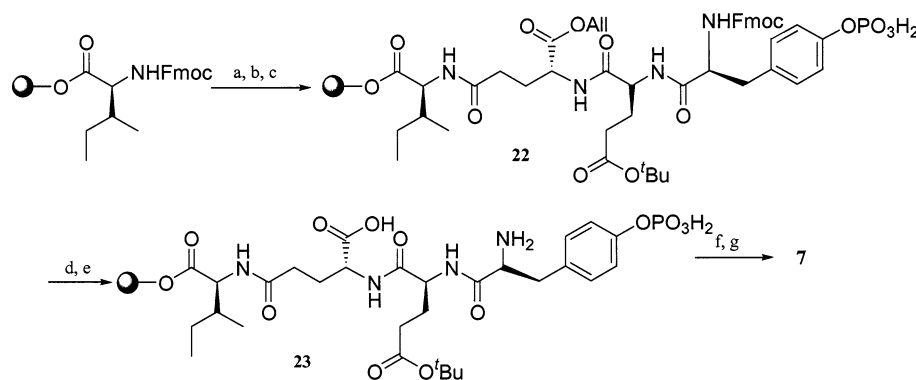
4.1. [pTyr-Glu]-Glu-Ile (Peptide 4): 2-(4-Carboxy-2-{[3,8-dioxo-2-(4-phosphonooxybenzyl)[1,4]diazocane-5-carbonyl]amino}butyrylamino)-3-methylpentanoic Acid. The resin-bound peptide **16** (0.1 mmol) (Scheme 1) was suspended in TFA/TIPS/DCM (1:5:94, 10 mL), mixed for 1 h, and filtered. This step was repeated, and the resin was collected by filtration and washed successively with TEA/DMF (1%, 50 mL), MeOH (50 mL), and DCM (50 mL). The *N*-Fmoc group was deprotected with 20% piperidine/DMF (2 × 5 min, 5 mL each time). After the mixture was washed with HCl/DMF (1%, 50 mL), MeOH (50 mL), and DCM (50 mL), the resin was collected by filtration and dried under vacuum overnight to give **17**. Cyclization of the resin-bound peptide **17** was carried out with a mixture of HBTU (300 mg, 0.8 mmol) and NMM (200 μL, 0.8 mmol) in dry DMF (5 mL) for 24 h, followed by cleavage of the peptide from the resin and HPLC purification as described above to yield compound **4** in an overall yield of 15%. ¹H NMR (400 MHz, CD₃OD) δ: 7.37 (2H, d, *J* = 8.2 Hz), 7.25 (2H, d, *J* = 8.2 Hz), 4.95–4.84 (1H, m), 4.58–4.42 (3H, m), 3.37 (2H, d, *J* = 7.7 Hz), 2.90–2.78 (1H, m), 2.52–2.32 (4H, m), 2.21–2.07 (2H, m), 2.05–1.90 (2H, m), 1.55–1.42 (2H, m), 1.35–1.21 (3H, m), 0.98 (3H, d, *J* = 6.72 Hz). ¹³C NMR (400 MHz, CD₃OD) δ: 181.1, 179.6, 177.1, 175.8, 174.3, 174.1, 132.5, 117.6, 61.8, 61.4, 55.6, 55.4, 41.2, 33.7, 30.5, 30.3, 28.3, 26.4, 24.4, 15.3, 12.9. HR-MS (ESI-TOF, M + H) *m/z* calculated for C₂₅H₃₆N₄O₁₂P 615.1989, found 615.1536.

4.2. [pTyr-Glu-Glu]-Ile (Peptide 5): 2-[5-(2-Carboxyethyl)-3,6,11-trioxo-2-(4-phosphonooxybenzyl)-1,4,7-triazacycloundecane-8-carbonyl]amino}-3-methylpentanoic Acid. This compound was synthesized in a similar manner

as described for peptide **4** with Fmoc-Glu(2-PhiPr)-OH assembled at the P + 2 position in the peptide sequence (Scheme 3). Cyclization of **21** was achieved with DPPA (diphenylphosphoryl azide, 10 equiv, 24 h). The peptide **5** (11% yield) was obtained after cleavage from the resin and purification using the HPLC method as described above in the general section. ¹H NMR (400 MHz, CD₃OD) δ: 7.17 (2H, d, *J* = 6.8 Hz), 7.05 (2H, d, *J* = 8.2 Hz), 4.91 (1H, t, *J* = 7.5 Hz), 4.45–4.38 (3H, m), 3.40 (2H, d, *J* = 7.5 Hz), 2.84–2.70 (1H, m), 2.40–2.23 (4H, m), 2.10–1.98 (2H, m), 1.95–1.75 (2H, m), 1.52–1.48 (2H, m), 1.22–1.07 (3H, m), 0.88 (3H, t, *J* = 7.5 Hz). HR-MS (ESI-TOF, M + H) *m/z* calculated for C₂₅H₃₆N₄O₁₂P 615.1989, found 615.3013.

4.3. [pTyr-γ-Glu]-Glu-Ile (Peptide 6): 2-(4-Carboxy-2-{3-[3,6-dioxo-5-(4-phosphonooxybenzyl)piperazin-2-yl]propionylamino}butyrylamino)-3-methylpentanoic Acid. The resin-bound peptide **18** (0.1 mmol) was suspended in a mixture of CHCl₃/AcOH/NMM (5 mL, 37:2:1), and Pd(Ph₃P)₄ (360 mg, 0.25 mmol) was added in one portion under dry nitrogen. The flask was wrapped in aluminum foil, and the resin was gently mixed for 2.5 h at room temperature. The resin was filtered and washed successively with TEA/DMF (1%, 50 mL), DMF (50 mL), MeOH (50 mL), and DCM (50 mL). The Fmoc group was then removed with 20% piperidine in DMF (2 × 5 min, 5 mL each time) to yield **19**. Cyclization of the resin-bound peptide **19** was achieved with the addition of two batches of HBTU/NMM (2 × 1.5 h, 4 equiv each time). Peptide **6** was cleaved from the resin and purified as described above in the general section in a moderate overall yield after cleavage (41%). ¹H NMR (400 MHz, CD₃OD) δ: 7.09 (2H, d, *J* = 7.7 Hz), 7.00 (2H, d, *J* = 7.7 Hz), 4.85 (1H, t, *J* = 7.2 Hz), 4.55–4.39 (3H, m), 3.34 (2H, d, *J* = 7.2 Hz), 2.88–2.75 (1H, m), 2.40 (2H, m), 2.37 (2H, m), 2.23 (2H, m), 2.09 (2H, m), 1.35 (2H, m), 1.12 (3H, d, *J* = 6.7 Hz), 0.98 (3H, t, *J* = 7.1 Hz). HR-MS (ESI-TOF, M + H) *m/z* calculated for C₂₅H₃₆N₄O₁₂P 615.1989, found 615.3121.

4.4. [pTyr-Glu-γ-Glu]-Ile (Peptide 7): 2-[3-[8-(2-Carboxyethyl)-3,6,9-trioxo-5-(4-phosphonooxybenzyl)[1,4,7-triazonan-2-yl]propionylamino}-3-methylpentanoic Acid. This compound was synthesized in a similar manner as described for peptide **6** with Fmoc-Glu-OAll assembled at the P + 2 position in the peptide sequence (Scheme 4). Cyclization of **23** was achieved with DPPA (20 equiv, 2 × 24 h). The peptide was cleaved from the resin and purified as described above in the general section in a low yield (ca. 7% based on the resin after cleavage). ¹H NMR (400 MHz, CD₃OD) δ: 7.24 (2H, d, *J* = 7.3 Hz), 7.17 (2H, d, *J* = 7.3 Hz), 4.62 (1H, m), 4.55–4.48 (3H, m), 3.38 (3H, m), 2.62 (1H, m), 2.45–2.37 (4H, m), 2.21–2.09 (4H, m), 1.44–1.39 (2H, m), 1.37–1.28 (3H, m), 0.96 (3H, d, *J* = 7.5 Hz). HR-MS (ESI-TOF, M + H) *m/z* calculated for C₂₅H₃₆N₄O₁₂P 615.1989, found 615.1922.

Scheme 4^a

^a Reagents: (a) (i) piperidine 20%/DMF; (ii) Fmoc-Glu-OAll, HBTU, NMM, DMF; (b) (i) piperidine 20%/DMF; (ii) Fmoc-Glu(*t*Bu)-OH, HBTU, NMM, DMF; (c) (i) piperidine 20%/DMF; (ii) Fmoc-Tyr(PO₃H₂)-OH, HBTU, NMM, DMF; (d) Pd(PPh₃)₄, CHCl₃/AcOH/NMM (37:2:1); (e) piperidine 20%/DMF; (f) DPPA (20 equiv, 2 × 24 h); (g) TFA/anisole/H₂O (90:5:5).

4.5. [pTyr-β-Asp]-Glu-Ile (Peptide 10): 2-(4-Carboxy-2-{2-[3,6-dioxo-5-(4-phosphonooxybenzyl)piperazin-2-yl]-acetyl-amino}butyrylamino)-3-methylpentanoic Acid. This compound was synthesized in a similar manner (7%) as for **6** with Fmoc-Asp-OAll used instead of Fmoc-Glu-OAll. ¹H NMR (400 MHz, CD₃OD) δ: 7.02 (2H, d, *J* = 8.2 Hz), 6.70 (2H, d, *J* = 8.2 Hz), 4.70 (1H, t, *J* = 6.8 Hz), 4.40 (2H, m), 3.40 (2H, m), 2.70 (1H, m), 2.55 (2H, m), 2.40 (2H, m), 2.22 (2H, m), 1.40 (2H, m), 1.15 (3H, m), 0.90 (3H, m). HR-MS (ESI-TOF, M + H) *m/z* calculated for C₂₄H₃₄N₄O₁₂P 601.1833, found 601.3111.

4.6. [pTyr-Glu-β-Asp]-Ile (Peptide 11): 2-{2-[8-(2-Carboxyethyl)-3,6,9-trioxo-5-(4-phosphonooxybenzyl)[1,4,7]-triazonan-2-yl]acetyl-amino}-3-methylpentanoic Acid. This compound was synthesized in a similar manner (10%) as for **7** with Fmoc-Asp-OAll used instead of Fmoc-Glu-OAll. ¹H NMR (400 MHz, CD₃OD) δ: 7.11 (2H, d, *J* = 8.8 Hz), 7.00 (2H, d, *J* = 8.8 Hz), 4.78 (1H, t, *J* = 7.2 Hz), 4.51–4.45 (2H, m), 3.42 (2H, m), 2.74–2.70 (1H, m), 2.51–2.42 (2H, m), 2.40–2.36 (2H, m), 2.29 (2H, m), 2.15 (2H, m), 1.41 (2H, m), 1.18 (3H, m), 0.96 (3H, m). HR-MS (ESI-TOF, M + H) *m/z* calculated for C₂₄H₃₄N₄O₁₂P 601.1833, found 601.1231.

5. Synthesis of Fluorescent Probe. The fluorescent probe was synthesized by coupling of 5-carboxyfluorescein succinimidyl ester with a pentapeptide (Gly-pTyr-Glu-Glu-Ile) containing the phosphotyrosine motif recognized by the Src SH2 domain and a glycine linker. Synthesis of 5-carboxyfluorescein succinimidyl ester and its coupling reaction with GpYEEI were carried out according to a previously reported procedure^{29,30} with some modifications as described below.

5.1. 5-Carboxyfluorescein Succinimidyl Ester. To a solution of 5-carboxyfluorescein (150 mg, 0.40 mmol, Sigma) in anhydrous DMF (1.5 mL) was added 1-[3-(dimethylamino)propyl]-3-ethylcarbodiimide hydrochloride (EDAC; 93.6 mg, 0.49 mmol, Acros Organics) followed by *N*-hydroxysuccinimide (HOSu; 57.4 mg, 0.50 mmol, Acros Organics). The reaction flask was covered with foil, and the solution was stirred under nitrogen for 4.5 h. After 4.5 h, additional EDAC (15.6 mg, 0.08 mmol) was added and the reaction mixture was stirred under nitrogen overnight. The reaction mixture was rinsed into a separatory funnel with a minimal amount of DMF and diluted with acetone (6.0 mL). K-phosphate buffer (0.1 M, pH 6, 7.5 mL) was added. The mixture was extracted with Et₂O/ethyl acetate (EtOAc) (2:1, 9.0 mL). The organic layer was separated, and the aqueous layer was extracted two times with Et₂O/EtOAc (2:1, 7.5 mL). The combined organic extracts were washed with water (3 × 6.0 mL) and brine (1 × 7.5 mL), dried over Na₂SO₄, and filtered. The organic solvents were removed in vacuo. A residue was dissolved in 2.0 mL of acetonitrile and purified by preparative HPLC as described above. The spectroscopic data were identical with those reported in literature.³⁰

5.2. Fluorescent Probe (5-Carboxyfluorescein-Gly-pTyr-Glu-Glu-Ile). The GpYEEI peptidyl resin and *N,N*-diisopropylethylamine (DIPEA; 850 μL, 6 equiv, Aldrich Chemical Company) were added to a solution of 5-carboxyfluorescein succinimidyl ester (250 mg, 0.53 mmol) in anhydrous DMF (5.0 mL). The mixture was stirred for 48 h at room temperature. The resin was filtered, washed with DMF (100 mL), and cleaved using a solution of TFA/water/trisopropyl silane (5.0 mL:0.5 mL:0.5 mL) for 2.5 h. The filtrate was collected, concentrated, precipitated from cold ether, and the crude product was purified by preparative reverse-phase HPLC as described above and analyzed by LC/MS and amino acid analysis. The analytical data were identical with those reported in literature.²⁹

Acknowledgment. We acknowledge the financial support from National Center for Research Resources, NIH, Grant No. 1 P20 RR16457, and Rhode Island Foundation, Grant No. 20030201.

References

- Luttrell, D. K.; Lee, A.; Lansing, T. J.; Crosby, R. M.; Jung, K. D.; Willard, D.; Luther, M.; Rodriguez, M.; Berman, J.; Gilmer, T. M. Involvement of pp60c-src with two major signaling pathways in human breast cancer. *Proc. Natl. Acad. Sci. U.S.A.* **1994**, *91*, 83–87.
- Boyce, B. F.; Yoneda, T.; Lowe, C.; Soriano, P.; Mundy, G. R. Requirement of pp60c-src expression for osteoclasts to form ruffled borders and resorb bone in mice. *J. Clin. Invest.* **1992**, *90*, 1622–1627.
- Soriano, P.; Montgomery, C.; Geske, R.; Bradley, A. Targeted disruption of the c-src proto-oncogene leads to osteopetrosis in mice. *Cell* **1991**, *64*, 693–702.
- Alonso, G.; Koegl, M.; Mazurenko, N.; Courtneidge, S. A. Sequence requirements for binding of Src family tyrosine kinases to activated growth factor receptors. *J. Biol. Chem.* **1995**, *270*, 9840–9848.
- Roussel, R. R.; Brodeur, S. R.; Shalloway, D.; Laudano, A. P. Selective binding of activated pp60c-src by an immobilized synthetic phosphopeptide modeled on the carboxyl terminus of pp60c-src. *Proc. Natl. Acad. Sci. U.S.A.* **1991**, *88*, 10696–10700.
- Payne, G.; Shoelson, S. E.; Gish, G. D.; Pawson, T.; Walsh, C. T. Kinetics of p56lck and p60src Src homology 2 domain binding to tyrosine-phosphorylated peptides determined by a competition assay or surface plasmon resonance. *Proc. Natl. Acad. Sci. U.S.A.* **1993**, *90*, 4902–4906.
- Payne, G.; Stolz, L. A.; Pei, D.; Band, H.; Shoelson, S. E.; Walsh, C. T. The phosphopeptide-binding specificity of Src family SH2 domains. *Chem. Biol.* **1994**, *1*, 99–105.
- Songyang, Z.; Shoelson, S. E.; Chaudhuri, M.; Gish, G.; Pawson, T.; Haser, W. G.; King, F.; Roberts, T.; Rutnoffsky, S.; Lechleider, R. J.; Neel, B. G.; Birge, R. B.; Fajardo, J. E.; Chou, M. M.; Hanafusa, H.; Schaffhausen, B.; Cantley, L. C. SH2 domains recognize specific phosphopeptide sequences. *Cell* **1993**, *72*, 767–778.

- (9) Waksman, G.; Shoelson, S. E.; Pant, N.; Cowburn, D.; Kuriyan, J. Binding of a high affinity phosphotyrosyl peptide to the Src SH2 domain: crystal structures of the complexed and peptide-free forms. *Cell* **1993**, *72*, 779–789.
- (10) Waksman, G.; Kominos, D.; Robertson, S. C.; Pant, N.; Baltimore, D.; Birge, R. B.; Cowburn, D.; Hanafusa, H.; Mayer, B. J.; Overduin, M.; Resh, M. D.; Rios, C. B.; Silverman, L.; Kuriyan, J. Crystal structure of the phosphotyrosine recognition domain SH2 of v-src complexed with tyrosine-phosphorylated peptides. *Nature* **1992**, *358*, 646–653.
- (11) Eck, M. J.; Shoelson, S. E.; Harrison, S. C. Recognition of a high-affinity phosphotyrosyl peptide by the Src homology-2 domain of p56lck. *Nature* **1993**, *362*, 87–91.
- (12) Lesuisse, D.; Deprez, P.; Albert, E.; Duc, T. T.; Sortais, B.; Gofflo, D.; Jean-Baptiste, V.; Marquette, J.; Schoot, B.; Sarubbi, E.; Lange, G.; Broto, P.; Mandine, E. Discovery of thioazepinone ligands for Src SH2: from non-specific to specific binding. *Bioorg. Med. Chem. Lett.* **2001**, *11*, 2127–2131.
- (13) Deprez, P.; Mandine, E.; Vermond, A.; Lesuisse, D. Imidazole-based ligands of the Src SH2 protein. *Bioorg. Med. Chem. Lett.* **2002**, *12*, 1287–1289.
- (14) Deprez, P.; Baholet, I.; Burlet, S.; Lange, G.; Amengual, R.; Schoot, B.; Vermond, A.; Mandine, E.; Lesuisse, D. Discovery of highly potent Src SH2 binders: Structure–activity studies and X-ray structures. *Bioorg. Med. Chem. Lett.* **2002**, *12*, 1291–1294.
- (15) Buchanan, J. L.; Bohacek, R. S.; Luke, G. P.; Hatada, M.; Lu, X.; Dalgarno, D. C.; Narula, S. S.; Yuan, R.; Holt, D. A. Structure-based design and synthesis of a novel class of Src SH2 inhibitors. *Bioorg. Med. Chem. Lett.* **1999**, *9*, 2353–2358.
- (16) Buchanan, J. L.; Vu, C. B.; Merry, T. J.; Corpuz, E. G.; Pradeepan, S. G.; Mani, U. N.; Yang, M.; Plake, H. R.; Varkhedkar, V. M.; Lynch, B. A.; MacNeil, I. A.; Loiacono, K. A.; Tiong, C. L.; Holt, D. A. Structure–activity relationships of a novel class of Src SH2 inhibitors. *Bioorg. Med. Chem. Lett.* **1999**, *9*, 2359–2364.
- (17) Humphrey, J. M.; Chamberlin, A. R. Chemical synthesis of natural product peptides: Coupling methods for the incorporation of noncoded amino acids into peptides. *Chem. Rev.* **1997**, *97*, 2243–2266.
- (18) Khan, A. R.; Parrish, J. C.; Fraser, M. E.; Smith, W. W.; Bartlett, P. A.; James, M. N. G. Lowering the entropic barrier for binding conformationally flexible inhibitors to enzymes. *Biochemistry* **1998**, *37*, 16839–16845.
- (19) Smith, W. W.; Bartlett, P. A. Macrocyclic inhibitors of penicillopepsin. 3. Design, synthesis, and evaluation of an inhibitor bridged between P2 and P1'. *J. Am. Chem. Soc.* **1998**, *120*, 4622–4628.
- (20) Davidson, J. P.; Lubman, O.; Rose, T.; Waksman, G.; Martin, S. F. Calorimetric and structural studies of 1,2,3-trisubstituted cyclopanes as conformationally constrained peptide inhibitors of Src SH2 domain binding. *J. Am. Chem. Soc.* **2002**, *124*, 205–215.
- (21) Etmayer, P.; France, D.; Gounarides, J.; Jarosinski, M.; Martin, M. S.; Rondeau, J. M.; Sabio, M.; Topiol, S.; Weidmann, B.; Zurini, M.; Bair, K. W. Structural and conformational requirements for high-affinity binding to the SH2 domain of Grb2. *J. Med. Chem.* **1999**, *42*, 971–980.
- (22) Lesuisse, D.; Lange, G.; Deprez, P.; Benard, D.; Schoot, B.; Delettre, G.; Marquette, J. P.; Broto, P.; Jean-Baptiste, V.; Bichet, P.; Sarubbi, E.; Mandine, E. SAR and X-ray. A new approach combining fragment-based screening and rational drug design: Application to the discovery of nanomolar inhibitors of Src SH2. *J. Med. Chem.* **2002**, *45*, 2379–2387.
- (23) Shakespeare, W.; Yang, M.; Bohacek, R.; Cerasoli, F.; Stebbins, K.; Sundaramoorthi, R.; Azimioara, M.; Vu, C.; Pradeepan, S.; Metcalf, C. C.; Haralson, C.; Merry, T.; Dalgarno, D.; Narula, S.; Hatada, M.; Lu, X.; van Schravendijk, M. R.; Adams, S.; Violette, S.; Smith, J.; Guan, W.; Bartlett, C.; Herson, J.; Iuliucci, J.; Weigle, M.; Sawyer, T. Structure-based design of an osteoclast-selective, nonpeptide Src homology 2 inhibitor with in vivo antiresorptive activity. *Proc. Natl. Acad. Sci. U.S.A.* **2000**, *97*, 9373–9378.
- (24) El Haddadi, M.; Cavelier, F.; Vives, E.; Azmani, A.; Verducci, J.; Martinez, J. All-L-Leu-Pro-Leu-Pro: a challenging cyclization. *J. Pept. Sci.* **2000**, *6*, 560–570.
- (25) Meutermans, W. D. F.; Bourne, G. T.; Golding, S. W.; Horton, D. A.; Campitelli, M. R.; Craik, D.; Scanlon, M.; Smythe, M. L. Difficult macrocyclizations: New strategies for synthesizing highly strained cyclic tetrapeptides. *Org. Lett.* **2003**, *5*, 2711–2714.
- (26) Yoon, U. C.; Jin, Y. X.; Oh, S. W.; Park, C. H.; Park, J. H.; Campana, C. F.; Cai, X.; Duesler, E. N.; Mariano, P. S. A synthetic strategy for the preparation of cyclic peptide mimetics based on SET-promoted photocyclization processes. *J. Am. Chem. Soc.* **2003**, *125*, 10664–10671.
- (27) Miranda, L. P.; Meutermans, W. D.; Smythe, M. L.; Alewood, P. F. An activated O → N acyl transfer auxiliary: efficient amide-backbone substitution of hindered “difficult” peptides. *J. Org. Chem.* **2000**, *65*, 5460–5468.
- (28) Meutermans, W. D. F.; Golding, S. W.; Bourne, G. T.; Miranda, L. P.; Dooley, M. J.; Alewood, P. F.; Smythe, M. L. Synthesis of difficult cyclic peptides by inclusion of a novel photolabile auxiliary in a ring contraction strategy. *J. Am. Chem. Soc.* **1999**, *121*, 9790–9796.
- (29) Lynch, B. A.; Loiacono, K. A.; Tiong, C. L.; Adams, S. E.; MacNeil, I. A. A fluorescence polarization based Src-SH2 binding assay. *Anal. Biochem.* **1997**, *247*, 77–82.
- (30) Adamczyk, M.; Fishpaugh, J. R.; Heuser, K. J. Preparation of succinimidyl and pentafluorophenyl active esters of 5- and 6-carboxyfluorescein. *Bioconjugate Chem.* **1997**, *8*, 253–255.
- (31) Kawahata, N. H.; Yang, M. H.; Luke, G. P.; Shakespeare, W. C.; Sundaramoorthi, R.; Wang, Y.; Johnson, D.; Merry, T.; Violette, S.; Guan, W.; Bartlett, C.; Smith, J.; Hatada, M.; Lu, X.; Dalgarno, D. C.; Eyermann, C. J.; Bohacek, R. S.; Sawyer, T. K. A novel phosphotyrosine mimetic 4'-carboxymethoxy-3'-phosphonophenylalanine (Cpp): exploitation in the design of nonpeptide inhibitors of pp60(Src) SH2 domain. *Bioorg. Med. Chem. Lett.* **2001**, *11*, 2319–2323.
- (32) Metcalf, C. A., III; van Schravendijk, M. R.; Dalgarno, D. C.; Sawyer, T. K. Targeting protein kinases for bone disease: discovery and development of Src inhibitors. *Curr. Pharm. Des.* **2002**, *8*, 2049–2075.
- (33) Burke, T. R., Jr.; Yao, Z. J.; Liu, D. G.; Voigt, J.; Gao, Y. Phosphoryltyrosyl mimetics in the design of peptide-based signal transduction inhibitors. *Biopolymers* **2001**, *60*, 32–44.
- (34) Burke, T. R., Jr.; Lee, K. Phosphotyrosyl mimetics in the development of signal transduction inhibitors. *Acc. Chem. Res.* **2003**, *36*, 424–433.

JM040008+